Supplemental Material for

Impaired hypocretin/orexin system alters responses to salient stimuli in obese male mice

Ying Tan[1,7,*], Fu Hang[1,8,*], Zhong-Wu Liu[1], Milan Stoiljkovic[1], Mingxing Wu[1,9], Yue Tu[1,10], Wenfei Han[2], Angela M Lee[3], Craig Kelley [4], Mihály Hajós[1], Lingeng Lu [5], Luis de Lecea[6], Ivan De Araujo[2], Marina R Picciotto[3], Tamas L Horvath[1] and Xiao-Bing Gao[1]

Departments of [1] Comparative Medicine and [3] Psychiatry, Yale University School of Medicine, [5] Department of Chronic Disease Epidemiology, Yale School of Public Health, New Haven, CT 06520, USA; [2] Department of Neuroscience, Icahn School of Medicine at Mount Sinai, New York City, NY 10029, USA; [4] SUNY Downstate/NYU Tandon, Joint Biomedical Engineering Program, Brooklyn, NY 11201, USA; [6] Department of Psychiatry and Behavioral Sciences, Stanford University School of Medicine, Palo Alto, CA 94304; [7] Department of Neurosurgery, Guizhou Provincial People's Hospital, Guiyang, Guizhou 550002, China; [8] Guangxi Reproductive Medical Research Center, First Affiliated Hospital of Guangxi Medical University, Nanning, Guangxi 530021, China; [9] Department of Ophthalmology, The Second Affiliate Hospital of Chongqing Medical University, Chongqing 400000, China; [10] Department of Traditional Chinese Medicine Health Preservation, Second Clinic Medical School, Nanjing University of Chinese Medicine, Nanjing, Jiangsu 210023, China. * Equal contribution

Conflict of interest statement: The authors have declared that no conflict of interest exists.

Correspondence to: Xiao-Bing Gao, Department of Comparative Medicine, Yale University School of Medicine, 333 Cedar St, New Haven, CT 06520. Phone 203 785-2340, Fax 203 737-1084, Email xiao-bing.gao@yale.edu

Supplemental Methods

Animals. C57BL/6J mice (4-6 months old) expressing green fluorescent protein (Hcrt-GFP) (1 - 4) or Cre-recombinase (Hcrt-Cre) (5) selectively in hypocretin neurons under the control of a specific hypocretin promoter were used in this study. Mice were group housed and maintained on a 12-12 hr light/dark cycle (lights on at 6:00 am) with free access to food and water under the care of Yale Animal Resources personnel.

Control and diet-induced obese (obese) mice. At an age of about 21 days old, male C57BL/6J mice were divided into two groups randomly: control, mice were fed with normal chow *ad lib* for 10-12 weeks; DIO, mice were fed with a high fat diet (HFD) with 45% of calorie from fat (D12451, Research Diets, Inc) *ad lib* for 10 -12 weeks. Only those mice in the obese group with a body weight gain > 100% were included in this study together with all animals in the control group. At 12 weeks on the diet, control and HFD-treated mice were scanned by nuclear magnetic resonance imaging (EchoMRI) in order to determine their whole-body composition.

Stereotaxic viral injections. The surgery for stereotaxic injection of AAV viral vector (rAAV5/EF1α-DIO-hM3Dq(Gq)-mCherry) was performed as reported by Han et al (6). Briefly, C57BL/6J mice at an age of 4-6 months, after 10-12 weeks of HFD treatment were anesthetized with isoflurane (as inhalant: 4% induction; 1-2% maintenance). Then, viral vectors were bilaterally injected into the LH using a Hamilton 1.0μL Neuros Model 7001KH syringe, at a rate of 0.02μL/min. The total volume of injection was 0.3 μL each side. The coordinates were: 1.46 mm caudal to Bregma and 1.1 mm lateral to midline and 5.0-5.4 mm below the skull surface. Preoperative analgesia with buprenorphine (0.05mg/Kg, *s.c.*) and postoperative analgesia with Carprofen (5mg/Kg, *s.c.*, twice per day for 3 consecutive days) were used. After surgery, mice were allowed to recover for at least two weeks before further experimental testing.

The expression of viral vectors was confirmed by dual immunocytochemical examinations of Hcrt and mCherry in injected mice.

Cocaine conditioned place preference (CPP). Cocaine CPP was performed as we reported previously (7). Briefly, C57BL/6J mice (male, *4-6 months old*) were transported in their home cages to the testing room about one hour before the first session and returned to the colony room at the end of the day. Baseline preference was measured on day 1 (at 12:30 PM) by allowing the mice to explore the CPP chambers freely for a total of 15 min. No baseline preference for either chamber was observed, and animals were then counter-balanced so that drug administration was randomly paired with one of the two training chambers. During the training phase (Days 2, 3, and 4), mice were injected (i.p.) with vehicle (saline) at 10:00 AM and confined for 30 min in one chamber. In the afternoon (3:00 PM), animals were isolated in the conditioning chamber following an injection of cocaine (3, 10 mg/kg, i.p.) or saline in control subjects. On day 5 (testing at 12:30 PM, chosen to be intermediate between saline and drug training times), animals were placed in the neutral compartment of the place conditioning apparatus, and were allowed free access to both conditioning chambers for 15 min. Total time spent in each chamber was recorded and a preference score was derived by calculating the difference between the time spent in the drug-paired chamber on the testing day (day 5) and the time spent in this same chamber at baseline (day 1). A decrease from baseline preference for the drug-paired chamber was considered as conditioned place aversion (CPA) while increased time in the chamber was interpreted as conditioned place preference (CPP). Preference scores obtained before (on day one) and after CPP training (day 5) were compared within each (control, obese and obese + DREADD) group and paired t-test was used.

Forced cold water swim (CWS). The forced cold water swim test was performed as reported elsewhere previously (8. 9). Briefly, C57BL/6J mice (male, *4-6 months old*) were put in a cylindrical container containing water at a temperature of 10ºC and a depth of 15 centimeters for 5 minutes and activities (swim

and immobilization) were monitored and recorded with video cameras for all animals. Immediately after the test, mice in all groups were removed from the cold water, carefully dried with a dry cotton towel and placed back into their home cages. Half of each cage was heated with a heating pad beneath the cage to keep the animals warm. Five minutes after the test, all animals were scarified under deep anesthesia followed by transcardial perfusion of fixative containing 4% paraformaldehyde in 0.1M sodium phosphate buffer (PB, pH 7.4). Brains were collected for the further immunocytochemical experiments as reported previously (3, 7).

Immunocytochemistry. Brains from all groups of animals collected in our study were cut into sections (50 μm thick) on a vibratome and were washed in a buffer containing 0.1% lysine, 1% BSA, 0.1% Tris, and 0.4% Triton X-100, after which they were blocked with 2% normal horse serum and were incubated overnight in primary antibodies for: orexin-B (Santa Cruz Biotechnology; sc-8071, goat, 1:2500) plus phospho-CREB (Ser133) (Cell Signaling Technology; # 9191, rabbit, 1:100) or AC3 (marker for primary cilium, Abcam ab125093, rabbit, 1:200). To test the expression of c-fos in Hcrt cells, primary antiserum against hypocretin (a gift from Dr. Anthony van den Pol's laboratory, rabbit, 1:1500) and primary antibody against c-fos (Santa Cruz Biotechnology; sc-52-G, goat, 1:1000) were used. After several washes with PB, sections were incubated in secondary antibodies (1:250) conjugated to Alexa Fluor 488 and 594 (Invitrogen) for 2-3 h. Specimens were examined with an FV 300 confocal laser scanning microscope (Olympus America, Melville, NY) or Keyence microscope system (Keyence Corp., Woburn, MA). For cell counting, at least 6 sections from each animal were taken at the level of the lateral hypothalamus, and the number of CREB/hypocretin positive neurons were counted and compared to the total number of hypocretin neurons. For the measurement of primary cilia in Hcrt cells, Z-scanning was performed along the whole depth of the cell and a 3-D reconstruction of Hcrt cells with primary cilia was performed with ImageJ. The lengths of primary cilia were presented as mean±S.E. for each group and Student's t-test was used to examine significance.

In vitro electrophysiology. Coronal hypothalamic slices, 300 μm thick, were cut from mice expressing GFP exclusively in Hcrt neurons as we reported previously (3, 4, 7). Briefly, mice were deeply anesthetized with isoflurane and decapitated, brains were rapidly removed and immersed in an oxygenated bath solution at 4°C containing (in mM): sucrose 220, KCl 2.5, $CaCl_2$ 1, $MgCl_2$ 6, NaH_2PO_4 1.25, $NaHCO_3$ 26, and glucose 10, pH 7.3 with NaOH. After preparation, slices were maintained in a holding chamber with artificial cerebrospinal fluid (ACSF) (bubbled with 5% CO_2 and 95% O_2) containing (in mM): NaCl 124, KCl 3, $CaCl_2$ 2, $MgCl_2$ 2, NaH_2PO_4 1.23, $NaHCO_3$ 26, glucose 10, pH 7.4 with NaOH, and were transferred to a recording chamber constantly perfused with a modified ACSF solution (with 2.5 mM glucose) (33 °C) at 2 ml/min after at least a 1 hr recovery.

Whole-cell voltage clamp (at -60 mV or at 0 mV) was performed to observe miniature excitatory and inhibitory postsynaptic currents with a Multiclamp 700A amplifier (Axon instrument, CA) as described previously (3, 4, 7). The patch pipettes with a tip resistance of 4-6 MΩ were made of borosilicate glass (World Precision Instruments) with a Sutter pipette puller (P-97) and filled with a pipette solution containing (in mM): K-gluconate (or Cs-gluconate as stated in the following sections) 135, $MgCl_2$ 2, HEPES 10, EGTA 1.1, Mg-ATP 2, Na_2-phosphocreatine 10, and Na_2-GTP 0.3, pH 7.3 with KOH. After a giga-ohm (GΩ) seal and whole-cell access were achieved, the series resistance (between 10 and 20 MΩ) was partially compensated by the amplifier. To monitor miniature mEPSCs and mIPSCs, voltage-dependent sodium channel blocker tetrodotoxin (TTX, 0.5 μM) was applied in the ACSF to eliminate the influence of action potentials on mEPSC and mIPSC events. To record mEPSCs and mIPSCs at different clamped membrane potentials in the same cells, Cs-gluconate but not K-gluconate was used in pipette solution to eliminate a large outward current due to the opening of potassium channels at 0 mV. To monitor evoked EPSCs, a bipolar tungsten electrode with a small distance of (50 μm) placed across an identified dendrite of Hcrt cells about 50 to 100 μm away from the soma where whole cell recording was performed. After a stable recording of eEPSCs was achieved, the stimulating intensity (20 to 50 μA) was adjusted to

trigger eEPSCs at about 30-50% of their maximal amplitudes. The stimulation and analysis of release probability were performed as reported by Thanawala and Regehr (10) with modifications. A train of high frequency stimulation (100 Hz, 50 pulses) was applied to the recorded cells in the presence of picrotoxin (300 nM). Cumulative amplitude of evoked EPSCs recorded from each cell was generated and normalized in tested cells. The linear regressions of the last 15 points of cumulative eEPSC was plotted and back extrapolated to the y-axis for each cell in both groups. The y-intercept corresponding to the effective readily releasable pool (eRRP) for that cell and the release probability was calculated as the quotient of the value of the first EPSC (normalized to the maximum value) divided by eRRP. In LTP experiments, a spike-timing dependent protocol was used as reported elsewhere (11, 12). Since action potential firing in Hcrt cells could run down rapidly due to the loss of intracellular contents during conventional whole cell recording with a low series resistance (10-20 MΩ) as reported previously by others and us (13, 14), we used a modified whole cell recording configuration with a high series resistance (30-40 MΩ) to eliminate the rundown of AP firing in Hcrt cells in this experiment by partially rupturing neuronal membrane after a gigaseal formation. In all experiments, only recordings with stable series resistance were accepted (the change in series resistance was less than 20%).

All data were sampled at 10 kHz and filtered at 3 kHz with an Apple Macintosh computer using AxoGraph X (developed by Dr. John Clements, AxoGraph, Inc.). Electrophysiological data were analyzed with AxoGraph X and plotted with Igor Pro software (WaveMetrics, Lake Oswego, OR). Specifically, mEPSC was analyzed with an event-detection package provided in AxoGraph X as reported previously (3, 4, 7). User-defined templates with characteristics of miniature synaptic events were slid along the signal to test for matches and the templates were automatically offset to adjust for baseline drift. An event was detected when the mismatch between a template and the signal approached the level of the recording noise. By using this approach, there was no need to filter the data and the default threshold setting usually gives excellent performance. Glitches and artifacts in the data were rejected because they do not conform to the template time course. Due to the variation in the recording condition among all cells, the parameters

for templates for mEPSC were as follows: rise time: 0.3 to 1 ms, decay time: 1 to 5 ms, amplitude: 10 to 20 pA. The parameters for templates for mIPSC were as follows: rise time: 0.5 to 5 ms, decay time: 5 to 20 ms, amplitude: 10 to 20 pA. The threshold for event detection was always 5 times of the noise standard error.

In vivo electrophysiology. Neurophysiological *in vivo* recordings were carried out in mice anesthetized with urethane (1.5 g/kg, i.p.) (15). After achieving a stable plane of anesthesia, which was controlled by the absence of a tail-pinch reflex, mice were placed in a Kopf stereotaxic frame (Tujunga, CA) on a temperature-regulated heating pad (Physitemp Instruments Inc., Clifton, NJ) set to maintain body temperature at 37-38 °C, and unilateral craniotomies were performed above the hypothalamus, hippocampus and rostral pons. After surgery, two bipolar concentric electrodes (NE-100X, Rhodes Medical Instruments, Woodland Hills, CA, USA) were inserted into lateral hypothalamic (1.5 mm posterior, 1.0 mm lateral and 4.7 mm dorsoventral) and hippocampal CA1 (2.0 mm posterior, 1.5 mm lateral and 1.5 mm dorsoventral) regions. Coordinates for each target area were taken from Paxinos and Franklin's mouse brain atlas, and referenced relative to Bregma and brain surface. Animals were allowed to stabilize before beginning of recording. 10 min after establishing the stable local field potentials (LFPs), they were intraperitoneally injected with saline (ND and HFD mice) or 0.3 mg/kg CNO (HFD-DREADD and HFD-CNO mice). The recording of spontaneous LFPs in the LH and CA1 started 20 min following injections of saline or CNO in each mouse and lasted for 15 minutes before initiation of elicited hippocampal oscillations by electrical stimulation of nPO as described previously (15). Briefly, the hypothalamic electrode was repositioned into the nPO (4.0 mm posterior, 1.2 mm lateral, and 3.3 mm dorsoventral), and stimulation consisted of a train of 0.3 ms square pulses delivered over a period of 6 seconds at a rate of 250 Hz and was repeated every 100 seconds using an Isoflex stimulus isolator unit (A.M.P.I. Instruments, Jerusalem, Israel). The stimulating current was increased stepwise from 0.0 to 0.2 mA in 0.02 mA increments and repeated in 3 cycles in order to establish a stimulus-response relationship

for both total power and peak frequency in theta band. The protocol for measuring evoked LFPs lasted for about 50 minutes. All recordings of spontaneous and evoked LFPs were performed within the effective time frame of CNO reported in mice (16 - 19). Throughout the duration of the experiment, mice were kept in the stereotaxic frame, spontaneous and stimulation-induced LFPs were continuously monitored, and the level of anesthesia regularly checked. At the conclusion of all recordings, animals were deeply anesthetized, transcardially perfused, and their brains removed for histological analysis.

In each experiment, LFPs were amplified and filtered between 1 and 300 Hz using Grass P55 AC differential amplifier (Grass Technologies, West Warwick, RI, USA) with an additional notch filter at 60 Hz. The signal was simultaneously sampled at a rate of 1 kHz and stored on a computer via a CED Micro1401-3 interface and Spike2 software (Cambridge Electronic Design, Cambridge, UK). For quantitative offline analyses, LFPs were subjected to Fast Fourier transform at a spectral resolution of 0.24 Hz. Computing stimulation-induced hippocampal theta power was done by summing power values between 3 Hz and 9 Hz, and peak frequency was identified by determining where the peak power occurred. To avoid possible stimulation artifacts, the first second of each 6-second long stimulation episode was omitted in all analyses. Total gamma power during spontaneous lateral hypothalamic and hippocampal activity was computed using the same method, except the signal was band-pass filtered between 30 Hz and 90 Hz. Theta phase-gamma amplitude coupling during hippocampal stimulation was assessed using modulation index (MI), as described previously (15, 20). Briefly, the phase containing signal from 3 to 10 Hz, and the amplitude containing signal from 20 to 100 Hz were used to calculate the MI value at each frequency pair for the maximal LFPs response recorded during each stimulation cycle.

Statistics. The software Prism 7 (GraphPad Software, Inc, La Jolla, CA) was used for statistical analyses. All data were initially determined to be suitable for parametric analysis according to normality and homoscedasticity. The comparison between two groups were examined with t-test, while comparison among three or more groups were examined with one-way random effects ANOVA except where

otherwise specified. The comparison of expression of LTP between control and DIO mice were performed with two-way ANOVA and *post hoc* Sidak's test. Statistical differences in the relationship between elicited theta power or peak frequency and current intensity were assessed by two-way ANOVA, while changes in spontaneous gamma power were tested with one-way ANOVA. For all post-hoc comparisons Tukey test was used. For statistical analyses of theta phase – gamma amplitude coupling in the hippocampus, the average MI in either low gamma (30 - 50 Hz) or high gamma (65 - 95 Hz) was calculated for each animal, grouped, and compared using a 2-tailed t test. Data are expressed as the mean ± standard error of the mean, and differences were considered significant when $p < 0.05$.

Study approval. All animal procedures were performed in strict accordance with NIH Care and Use of Laboratory Animals Guidelines and were approved by the Yale University Animal Care and Use Committee.

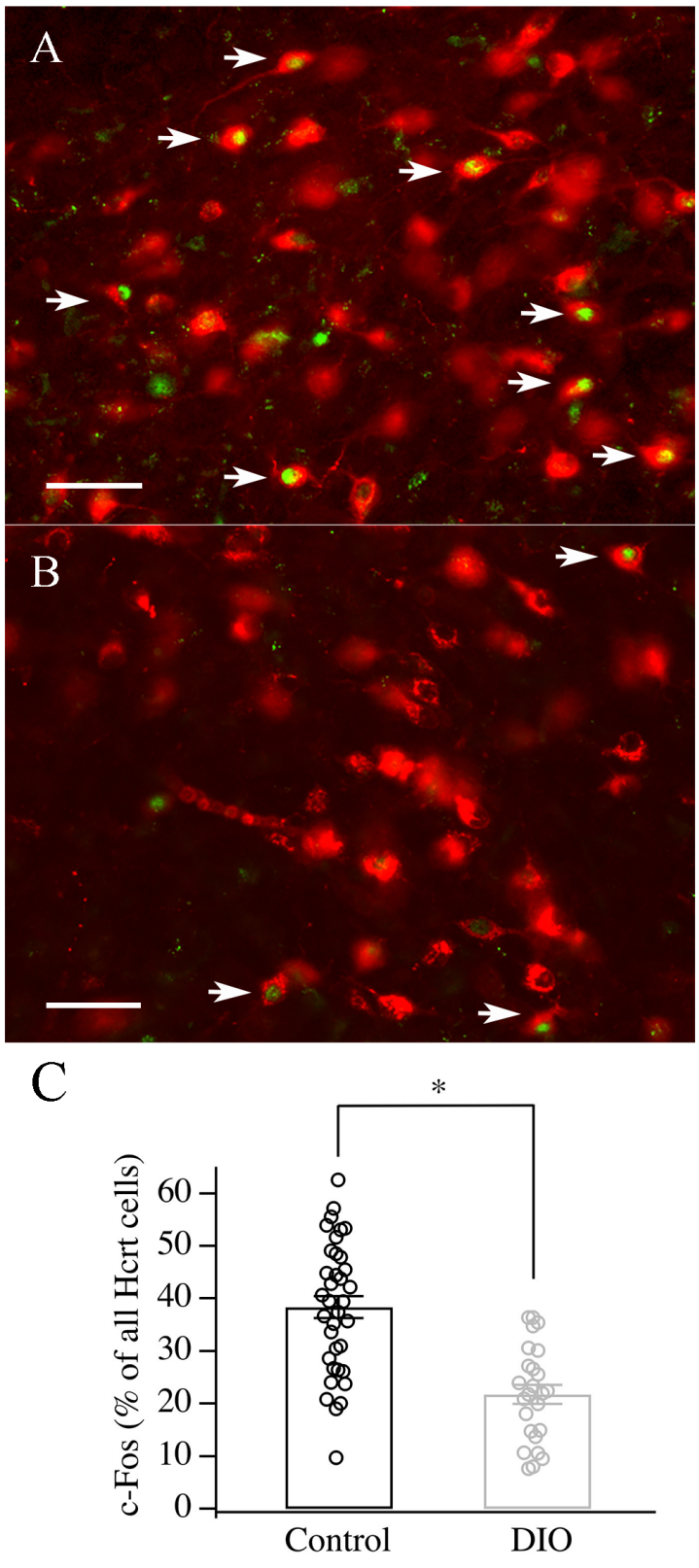

Supplemental Figure 1. The expression of c-Fos in Hcrt neurons induced by an acute administration of low dose cocaine (3 mg/kg, i.p.) in home cages was significantly lower in DIO mice (B) than in controls

(A). Scale bar: 50 μm. C57BL/6J mice at 3-4 weeks of age were divided into control and DIO groups. After 12 weeks of diet treatments, all mice were administrated one dose of cocaine (3 mg/kg, i.p.) and sacrificed 90 minutes later for the examination of c-Fos expressions (Green) in Hcrt neurons (Red) by dual-immunocytochemistry. Our data revealed that the percentage of Hcrt neurons with positive nuclear c-Fos immunoreaction was 38.3 ± 2.1% (n = 36 samples from 4 mice) and 21.8 ± 1.8% (n = 25 samples from 4 mice) in control and DIO groups, respectively. The c-Fos expression was significantly lower in Hcrt neurons in DIO mice than in the control group ($t = 5.643$, $df = 59$, $P < 0.0001$, two-tailed t-test).

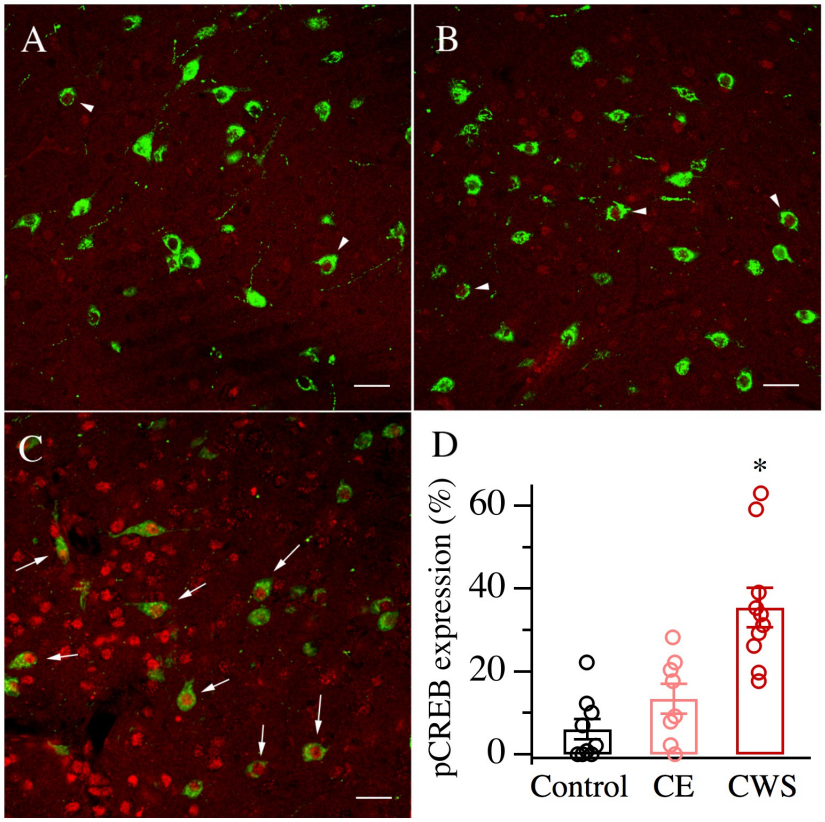

Supplemental Figure 2. The phosphorylation of CREB in Hcrt neurons significantly increased in mice undergoing forced swim in cold water (C) but not in mice only being exposed to cold water only (B) as compared with the control group (A). Scale bar: 30 μm. C57BL/6J mice at 4-6 weeks of age were divided into three groups: control, mice were placed in an empty cylindrical container; cold water exposure (CE), mice were put in a cylindrical container containing a shallow cold water with a depth of 2.5 centimeters; and cold-water swim (CWS), mice were put in a cylindrical container containing cold water with a depth of 15 centimeters and mice had to swim. The CE group was used to examine whether the exposure to cold water alone activates Hcrt neurons or not. All mice were sacrificed 30 minutes later followed by examination of pCREB expressions in Hcrt neurons by dual-immunocytochemistry. Our data revealed that the percentage of Hcrt neurons with positive nuclear pCREB immunoreaction was 6.0 ± 2.5% (n = 9 mice), 13.4 ± 3.6% (n = 8 mice) and 35.4 ± 4.8% (n = 10 mice) in control, CE and CWS groups, respectively. The pCREB expression was significantly higher in Hcrt neurons in CWS mice than in the other two groups ($F(2, 24) = 16.57$, $P<0.0001$, one-way ANOVA; *Post hoc Tukey's test*: control vs. CE,

q = 1.862, df = 24, p = 0.401; control vs. CWS, q = 7.801, df = 24, p < 0.0001; CE vs. CWS, q = 5.649, df = 24, p = 0.0015).

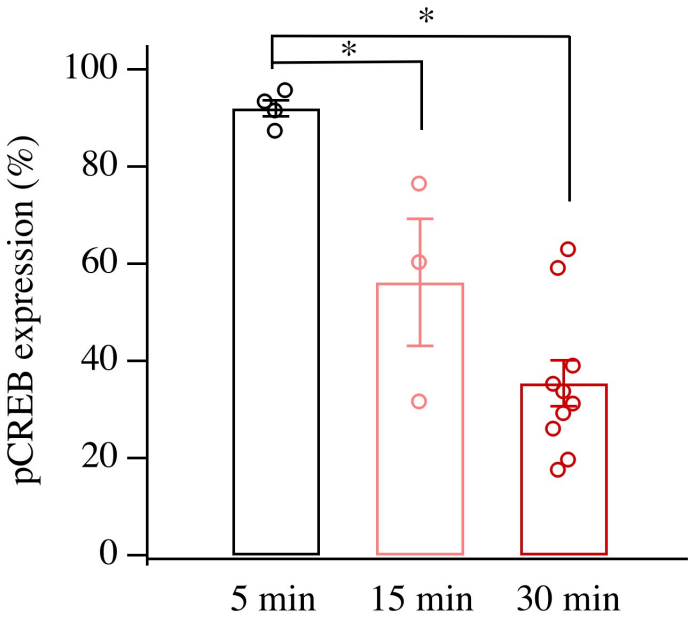

Supplemental Figure 3. The time course of the expression of pCREB in Hcrt cells after CWS exposure. C57BL/6J mice (male, 4-6 weeks old) were sacrificed 5, 15 and 30 minutes after a 5-min CWS episode for the examination of pCREB expressions in Hcrt neurons by dual-immunocytochemistry. The percentage expression of pCREB in the total number of Hcrt cells was 92.1 ± 1.8 % (n= 4 mice), 56.2 ±13.1 % (n=3 mice) and 35.4 ± 4.8 % (n=10 mice) at 5, 15 and 30 minutes after CWS, respectively. The difference was significant ($F(2, 14) = 20.73$, $P<0.0001$, one-way ANOVA; *Post hoc Tuckey's test*: 5 min vs. 15 min, $q = 4.451$, $df = 14$, $p = 0.0183$; 5 min vs. 30 min, $q = 9.08$, $df = 14$, $p < 0.0001$; 15 min vs. 30 min, $q = 2.995$, $df = 14$, $p = 0.1220$). Therefore, the time point of 5 minutes after CWS exposure was used in this study.

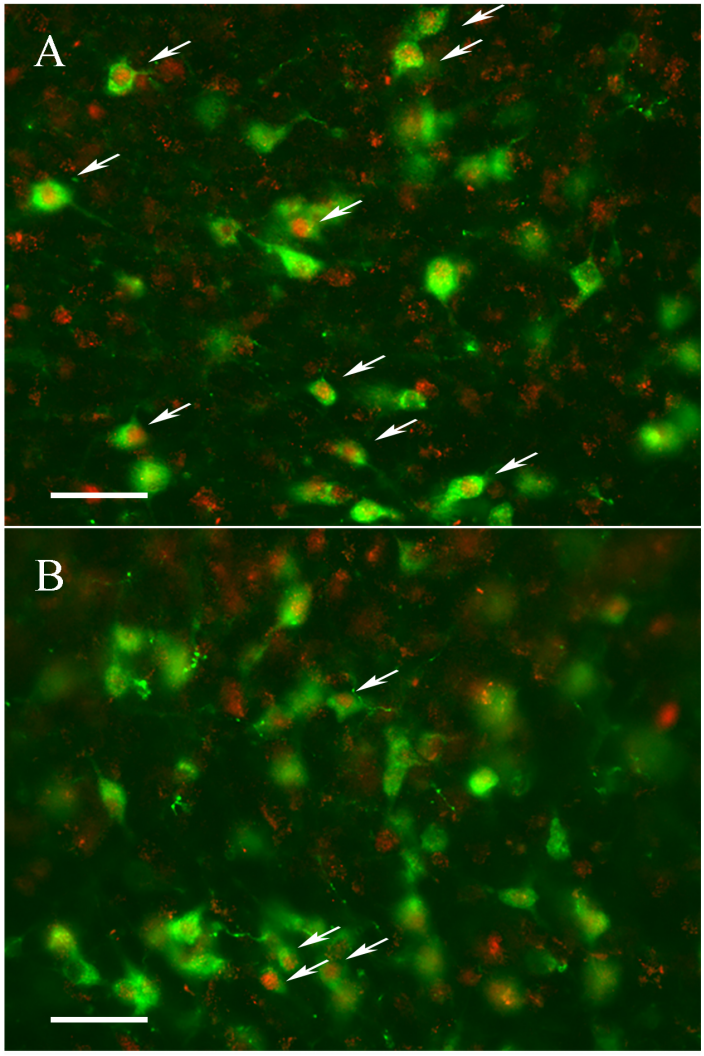

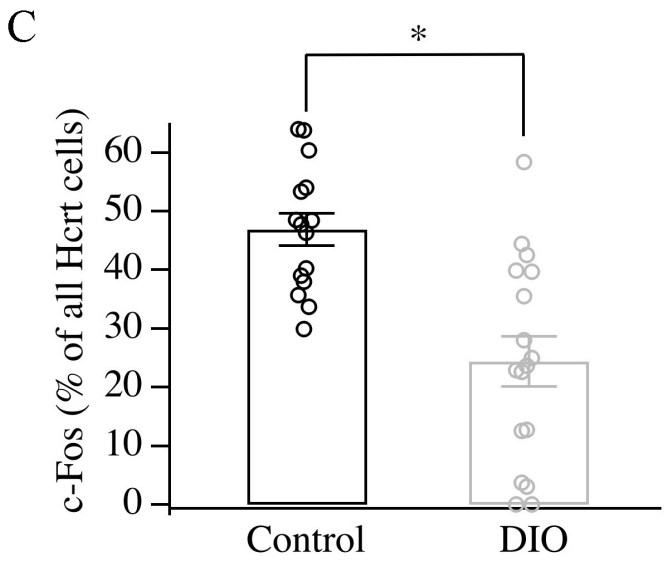

Supplemental Figure 4. The expression of c-Fos in Hcrt neurons induced by an acute CWS exposure was significantly lower in DIO mice (B) than in controls (A). Scale bar: 50 μm. C57BL/6J mice at 3-4

weeks of age were divided into control and DIO groups. After 12 weeks of diet treatments, all mice were exposed to CWS test and sacrificed 90 minutes later followed by examination of c-Fos expressions (Red) in Hcrt neurons (Green) using dual-immunocytochemistry. Our data revealed that the percentage of Hcrt neurons with positive nuclear c-Fos immunoreaction was 46.8 ± 2.8% (n = 15 samples from 4 mice) and 24.4 ± 4.2% (n = 17 samples from 4 mice) in control and DIO groups, respectively. The c-Fos expression was significantly lower in Hcrt neurons in DIO mice than in the control group ($t = 4.314$, $df = 30$, $P < 0.0001$, two-tailed t-test).

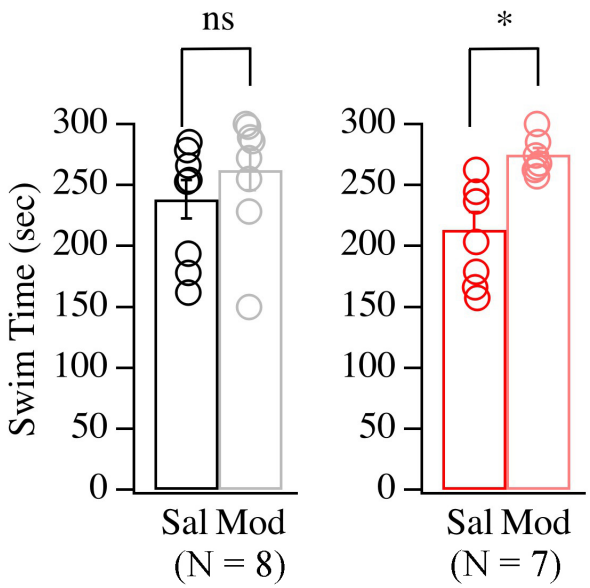

Supplemental Figure 5. An enhancement of arousal rescued the decreased time spent in swim during the forced cold-water swim test in obese mice. Bar graph showing the time spent in swim during a 5-min forced cold water swim test in control (left) and obese (DIO, right) mice. Forced cold water swim was performed 30 minutes after the administration of saline (Sal, i.p.) or modafinil (Mod, 20 mg/kg, i.p.) in control and obese mice. * $P<0.05$, two-tailed t-test.

Supplemental References:

1. Horvath TL, Gao XB. Input organization and plasticity of hypocretin neurons: possible clues to obesity's association with insomnia. *Cell Metab* 2005; 1: 279-286.
2. Li Y, Gao XB, Sakurai T, van den Pol AN. Hypocretin/Orexin excites hypocretin neurons via a local glutamate neuron-A potential mechanism for orchestrating the hypothalamic arousal system. Neuron. 2002; 36(6):1169-81.
3. Rao Y, et al. Regulation of synaptic efficacy in hypocretin/orexin-containing neurons by melanin concentrating hormone in the lateral hypothalamus. J Neurosci. 2008; 28(37):9101-10.
4. Rao Y, et al. Prolonged wakefulness induces experience-dependent synaptic plasticity in mouse hypocretin/orexin neurons. J Clin Invest. 2007; 117(12): 4022-33.
5. Giardino WJ, Eban-Rothschild A, Christoffel DJ, Li S-B, Malenka RC, de Lecea L. Parallel circuits from the bed nuclei of stria terminalis to the lateral hypothalamus drive opposing emotional states. Nat Neurosci. 2018; 21: 1084–1095.
6. Han W, et al. A Neural Circuit for Gut-Induced Reward. Cell. 2018; 175: 665-678.
7. Rao Y, et al. Repeated in vivo exposure of cocaine induces long-lasting synaptic plasticity in hypocretin/orexin-producing neurons in the lateral hypothalamus in mice. J Physiol. 2013; 591: 1951-66.
8. Campioni MR, Xu M, McGehee DS. Stress-induced changes in nucleus accumbens glutamate synaptic plasticity. J Neurophysiol. 2009; 101: 3192-8.
9. Wang Q, Wang M, Whim MD. Neuropeptide y gates a stress-induced, long-lasting plasticity in the sympathetic nervous system. J Neurosci. 2013; 33: 12705-17.
10. Thanawala MS, Regehr WG. Presynaptic calcium influx controls neurotransmitter release in part by regulating the effective size of the readily releasable pool. J Neurosci. 2013; 33(11):4625-33.
11. Liu QS, Pu L, Poo MM. Repeated cocaine exposure in vivo facilitates LTP induction in midbrain dopamine neurons. Nature. 2005; 437(7061):1027-31.
12. Dietrich MO, et al. AgRP neurons regulate development of dopamine neuronal plasticity and nonfood-associated behaviors. Nat Neurosci. 2012; 15(8):1108-10.
13. Parsons MP, Hirasawa M. ATP-sensitive potassium channel-mediated lactate effect on orexin neurons: implications for brain energetics during arousal. J Neurosci. 2010; 30: 8061–8070.
14. Liu ZW, Gan G, Suyama S, Gao XB. Intracellular energy status regulates activity in hypocretin/orexin neurones: a link between energy and behavioural states. J Physiol. 2011; 589:4157–4166.
15. Stoiljkovic M, et al. Hippocampal network dynamics in response to α7 nACh receptors activation in amyloid-β overproducing transgenic mice. Neurobiol Aging. 2016; 45:161–168.

16. Weiss J, Nakajima K, Jain S. Novel designer receptors to probe GPCR signaling and physiology. Trends in pharmacological sciences. 2013; 34: 385-392.
17. Alexander GM, et al. Remote control of neuronal activity in transgenic mice expressing evolved G protein-coupled receptors. Neuron. 2009: 63: 27-39.
18. Sasaki K, Suzuki M, Mieda M, Tsujino N, Roth B, Sakurai T. Pharmacogenetic modulation of orexin neurons alters sleep/wakefulness states in mice. PloS One. 2011; 6: e20360.
19. Purohit K, et al. Pharmacogenetic manipulation of the nucleus accumbens alters binge-like alcohol drinking in mice. Alcoholism: Clinical and Experimental Research. 2018; 42: 879-888.
20. Tort AB, Komorowski RW, Manns JR, Kopell NJ, Eichenbaum H. Theta-gamma coupling increases during the learning of item-context associations. Proc Natl Acad Sci USA. 2009; 106: 20942–20947.